American Mineralogist, Volume 71, pages 547–556, 1986

High-temperature structure and crystal chemistry of hydrous alkali-rich beryl from the Harding pegmatite, Taos County, New Mexico

GORDON E. BROWN, JR., BRADFORD A. MILLS[1]
Department of Geology, Stanford University, Stanford, California 94305

ABSTRACT

The structure of hydrous Li-, Cs-, and Na-rich beryl from the Harding, New Mexico, pegmatite has been refined to an R factor of 0.050 using single-crystal X-ray methods. Alkali ions plus water molecules were located by difference Fourier methods in two sites within the channels paralleling c. Orientation of water molecules was determined from polarized IR spectra. The resulting structural formula is

$$[W(I)_{0.09}W(II)_{0.46}Cs_{0.09}K_{0.05}\square_{0.31}]^{XII}[Na_{0.21}Ca_{0.02}Mg_{0.02}Fe^{3+}_{0.01}\square_{0.74}]^{VI}$$
$$[Al_{2.0}]^{VI}[Be_{2.59}Li_{0.38}Al_{0.02}]^{IV}[Si_{5.92}Al_{0.08}]^{IV}O_{18},$$

where W(I) and W(II) represent Type I (H-H vector parallel to c) and Type II (H-H vector perpendicular to c) water, respectively, and □ represents vacancies. Li occupies the nonring tetrahedral site; water molecules, Cs, and K occupy the 12-coordinated channel site between six-membered silicate rings; and Na and Ca occupy the six-coordinated channel site within the rings.

The structure was also refined at 500, 800, and 24°C, after heating, and cell parameters were determined at 200, 300, 400, 500, 600, 700, and 800°C. The a and c cell parameters were found to expand over this temperature range with the following coefficients: $\epsilon_1 = 1.2 \times 10^{-6}$ °C^{-1} and $\epsilon_3 = 3.1\text{–}1.5 \times 10^{-6}$ °C^{-1}. The thermal expansion is consistent with changes in Gruneisen parameters, γ_1 and γ_3, with increasing temperature and can be rationalized in terms of (1) increases in volume of AlO_6 octahedra and $(Be,Li)O_4$ tetrahedra, (2) changes in T–O–Al and O–T–O angles (T = Si,Be,Li,Al), (3) rotation of $(Be,Li)O_4$ tetrahedra about axes lying in (001), and (4) rotation of vertically adjacent six-membered rings in opposite senses about [001]. Our results contrast with the thermal expansion of nonalkali hydrous and anhydrous synthetic beryl, emerald, and low-alkali hydrous cordierite. Heat treatment at 800°C for 72 h had little effect on the occupancies of channel sites; little dehydration occurred because the large alkali ions effectively plug the channels.

INTRODUCTION

Beryl is a beryllium aluminum silicate mineral often found in granitic pegmatites in which it can occur as free-standing, euhedral crystals in "pockets" or as "frozen," anhedral to euhedral crystals associated in either case with quartz, K-feldspar, albite, muscovite, and a variety of accessory minerals. The beryl structure, illustrated schematically in Figure 1, consists of six-membered rings of silica tetrahedra cross-linked by Be-containing tetrahedra and Al-containing octahedra to form a tetrahedral framework with open channels that parallel the c axis (Gibbs et al., 1968). Pegmatitic beryls commonly contain varying amounts of alkali-metal cations as well as alkaline earths, Fe, and other cations. Studies of compositional variations (see, e.g., Filho et al., 1973) and structural details (Evans and Mrose, 1968; Gibbs et al., 1968; Bakakin et al., 1969; Hawthorne and Černý, 1977; Price et al., 1976; Goldman et al., 1978; Aines and Rossman, 1984) have shown that the open channels in the beryl structure can accommodate these cations and water molecules similar to the channels in cordierite (Hochella et al., 1979; Goldman et al., 1977; Carson et al., 1982).

The present study is concerned with the structure and crystal chemistry of a high-alkali beryl that occurred as a euhedral crystal "frozen" or included within a smoky quartz vein in the microcline-spodumene-lepidolite-albite-muscovite-quartz core zone of the Harding pegmatite in Taos County, New Mexico (Jahns and Ewing, 1976, 1977). Considering Hawthorne and Černý's (1977) structural study of a Li- and Cs-rich beryl from the Tanco (Manitoba) pegmatite, our independent results on Li-Cs substitution in beryl are discussed only briefly, and the major emphasis is placed on (1) response of the beryl structure to temperature, (2) the role of channel constituents in the thermal expansion behavior of beryl, and (3)

[1] Present address: CR Exploration, 755 Gregg Street, Sparks, Nevada 89431.

0003–004X/86/0304–0547$02.00

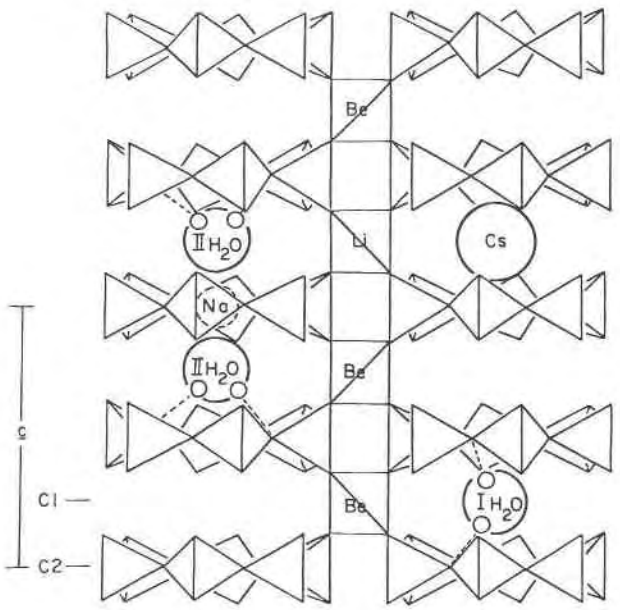

Fig. 1. Schematic illustration of the beryl structure showing the hexagonal rings of Si tetrahedra, designated T1, linked by Be and Li tetrahedra, designated T2. Possible positions for channel constituents are also shown, although *P6/mcc* symmetry must be obeyed, on the average.

comparison of the structure and thermal expansion of beryl and cordierite.

Experimental details

A specimen of beryl from the Harding pegmatite was kindly provided for this study by the late R. H. Jahns of Stanford University. This particular specimen was selected for structural study because an earlier wet chemical analysis (Table 1) showed it to be enriched in alkalis relative to other available, chemically homogeneous, pegmatitic beryls. A polished section examined by electron microprobe was found to be chemically homogeneous,

Table 1. Chemical analysis of Harding beryl HB-3[1]

Oxide	Wt. %	Normalized %	Atomic Proportion	No. Cations/18 Oxygens
SiO_2	62.88	63.88	1.063	5.92
BeO	11.43	11.61	.464	2.59
Al_2O_3	18.92	19.22	.188	2.10
Fe_2O_3	0.12	0.12	.001	0.01
FeO	...	...	...	...
MnO	tr.	...	...	...
MgO	0.17	0.17	.004	0.02
TiO_2	0.03	0.03	...	...
Li_2O	0.99	1.01	.034	0.38
Na_2O	1.13	1.15	.018	0.21
K_2O	0.38	0.39	.004	0.05
Cs_2O	2.21	2.24	.008	0.09
CaO	0.18	0.18	.003	0.02
H_2O	1.74	0.00	.098	0.55
Total	100.18	100.00	...	...

[1]*Analysis by L. E. Peck and R. E. Stevens.*

[2]*Oxide weight percent normalized to 100% after excluding* H_2O *(See Schaller,* et al. *[1962]).*

Table 2. Cell parameters of beryl HB-3 at eight temperatures

Temperature (°C)	a(Å)	c(Å)	V(Å^3)
24°	9.236(1)[1]	9.246(1)	683.0(2)
200°	9.241(1)	9.252(1)	684.2(2)
300°	9.244(1)	9.253(1)	684.7(2)
400°	9.249(1)	9.257(1)	685.8(2)
500°	9.251(1)	9.260(1)	686.3(2)
500° [2]	9.246(1)	9.254(1)	685.1(2)
600°	9.253(1)	9.259(1)	686.5(2)
700°	9.256(1)	9.262(1)	687.2(2)
800°	9.259(1)	9.264(1)	687.8(2)
500° [3]	9.245(1)	9.252(1)	684.8(2)
24° [3]	9.233(1)	9.243(1)	682.4(2)

[1]*Numbers in parentheses represent the estimated standard error (1$\hat{\sigma}$) in the last decimal place.*

[2]*After 96 hours.*

[3]*After heating.*

with the possible exception of Li and Be, which were not detectable. Our microprobe analysis is consistent with the composition in Table 1. A clear fragment designated HB-3 and measuring 0.12 × 0.12 × 0.20 mm was examined by precession photography; precession photographs displayed Laue symmetry D_{6h} and systematic absences of the type *hhl,* and *h0l, l* odd, which are consistent with space-group symmetry *P6/mcc.* The crystal was remounted in high-temperature mullite cement and sealed in an evacuated silica-glass capillary. The c axis was oriented parallel to the rotation axis of the goniometer head, and the crystal was transferred to a Picker FACS-I X-ray diffractometer equipped with a furnace (Brown et al., 1973). The furnace was calibrated to 1000°C by observing the beginning of melting of 200-μm diameter crystals of five standard compounds placed in evacuated silica-glass capillary tubes. Cell parameters (Table 2) were obtained by least-squares refinement of the angular settings of 28 automatically centered reflections in the 2θ range 30°–50°.

Intensity data were gathered at 24°C using graphite-monochromatized Mo K_α radiation (36 kV, 16 mA) and a take-off angle of 2.5°. Approximately 500 symmetry-independent reflections within the 2θ range 5°–65° were collected by using the θ–2θ scan technique, a scan rate of 1° 2θ per minute, and a scan range of 2.5° plus the $\alpha_1 - \alpha_2$ dispersion. Background radiation was recorded for 10 s at the high- and low-angle ends of each scan. Two standard reflections (500, 006) were measured every 27 reflections to check crystal alignment and electronic fluctuations, both of which proved to be negligible over the course of the experiment.

Cell dimensions were measured at 24, 200, 300, 400, and 500°C in the same manner as for the 24°C cell determination. During automatic centering of reflections and intensity measurements at temperature, crystal temperature was recorded continuously using a strip chart recorder and varied less than ±10°C.

Intensity data were gathered at 500°C using the orientation matrix determined from the auto-centering experiment at 500°C. Experimental parameters during data collection at high temperature were the same as those for the 24°C data set. Cell dimensions were determined again at 500°C, after the 96 h required for intensity data to be collected at that temperature, and were subsequently determined at 600, 700, and 800°C. A third set of intensity data was collected at 800°C after the crystal was equilibrated at this temperature for 72 h. Subsequently, cell parameters were determined at 500 and 24°C. A final set of intensity data was collected at 24°C in order to determine the effects of prolonged heating.

Table 3. Refinement parameters for beryl HB-3 at three temperatures

Parameter	24°C	500°C	800°C	24°C[1]
No. least-squared variables	31	31	31	31
Total No. non-equivalent reflections	508	447	427	473
No. reflections[2]	395	352	329	412
R[3]	0.050	0.093	0.070	0.053
R (weighted)[4]	0.049	0.077	0.058	0.050
$\hat{\sigma}$ (unit weight observation)	1.63	2.23	1.74	1.65

[1] *After heating.*

[2] *Included in final cycle of refinement. Reflections with* $F < 3\hat{\sigma}(F)$ *or with* $|F_o - F_c| > 10$ *were rejected. There were no more than 3 reflections satisfying the latter condition in each refinement.*

[3] $R = \Sigma(|F_o| - |F_c|)/\Sigma|F_o|$

[4] $R\ (wt.) = \Sigma w(|F_o| - |F_c|)^2/\Sigma w F_o^2]^{1/2}$

Intensity data were corrected for Lorentz and polarization effects, assuming a 50% ideally mosaic monochromator crystal. Because of the relatively small crystal size and low linear absorption coefficient ($\mu = 11.26$ cm^{-1}), no absorption correction was applied; differential absorption due to differences in transmission ranged from 0.80 to 0.87. Standard deviations were estimated by using the formula suggested by Corfield et al. (1967) with a diffractometer factor of 0.04. Refinement of the 24, 500, 800, and final 24°C structures was initiated in space group *P6/mcc* by using the coordinates of Gibbs et al. (1968), neutral atomic scattering factors from Doyle and Turner (1968), and anomalous dispersion corrections from MacGillavry and Rieck (1968). The program RFINE (Finger and Prince, 1975) was employed, a secondary extinction correction was refined, and weights based on counting statistics were assumed. Reflections with $F < 3\hat{\sigma}(F)$ were considered unobserved and were not used. Moreover, reflections for which calculated and observed structure factors differed by more than an arbitrary value of $\Delta F = 10.0$ were not included in the refinement, though no more than three of these were found in any given data set.

Difference Fourier maps, computed after refinement of the 24°C data set by using A. Zalkin's unpublished FORDAP program, indicated electron density at two positions within the channels, C(1): (0, 0, ¼) and C(2): (0, 0, 0); the density at C(1) was approximately four times greater than that at C(2). Cs, K, and H_2O were assigned to the larger C(1) site, whereas Na and the small amounts of Ca, Mg, and Fe^{3+} were assigned to the smaller C(2) site, resulting in essentially featureless electron-density difference maps at these sites. Li was assigned to the Be tetrahedral site after the models of Bakakin et al. (1969) and Hawthorne and Černý (1977). Least-squares refinements of all data sets converged rapidly to the *R* factors listed in Table 3, and final positional and thermal parameters are listed in Table 4. Selected interatomic distances and angles calculated using L. W. Finger's unpublished program ERROR are listed in Table 5, and observed and calculated structure factors for all four data sets are given in Table 6.[2]

[2] To receive a copy of Table 6, order Document AM-86-299 from the Business Office, Mineralogical Society of America, 1625 I Street, N.W., Suite 414, Washington, D.C. 20006. Please remit $5.00 in advance for the microfiche.

Table 4. Refined positional and thermal parameters for beryl HB-3 at three temperatures

Atom	Parameter	24°C	500°C	800°C	24°C[1]
T2	x	0.50	0.50	0.50	0.50
	y	0.00	0.00	0.00	0.00
	z	0.25	0.25	0.25	0.25
	β_{11}	0.0033(7)[2]	0.0018(10)	0.0064(14)	0.0021(6)
	β_{22}	0.0025(10)	0.0198(34)	-.0025(9)	0.0026(9)
	β_{33}	0.0031(7)	0.0035(14)	0.0062(13)	0.0018(5)
	β_{12}	½β_{22}	½β_{22}	½β_{22}	½β_{22}
	B(eq)[3]	0.88(10)	2.20(31)	2.01(16)	0.59(9)
M	x	0.6667	0.6667	0.6667	0.6667
	y	0.3333	0.3333	0.3333	0.3333
	z	0.25	0.25	0.25	0.25
	β_{11}	0.0015(2)	0.0041(4)	0.0046(3)	0.0017(1)
	β_{22}	β_{11}	β_{11}	β_{11}	β_{11}
	β_{33}	0.0012(2)	0.0031(4)	0.0027(3)	0.0017(2)
	β_{12}	½β_{11}	½β_{11}	½β_{11}	½β_{11}
	B(eq)	0.38(3)	1.05(7)	1.09(5)	0.48(3)
T1	x	0.3893(2)	0.3892(3)	0.3886(2)	0.3891(2)
	y	0.1189(2)	0.1194(3)	0.1183(2)	0.1186(2)
	z	0.00	0.00	0.00	0.00
	β_{11}	0.0011(1)	0.0019(3)	0.0032(2)	0.0013(1)
	β_{22}	0.0014(2)	0.0025(3)	0.0038(3)	0.0012(2)
	β_{33}	0.0013(1)	0.0025(2)	0.0027(2)	0.0014(1)
	β_{12}	0.0007(1)	0.0012(3)	0.0018(2)	0.0006(1)
	B(eq)	0.36(2)	0.65(4)	0.91(3)	0.37(2)
O1	x	0.3057(4)	0.3039(9)	0.3042(7)	0.3055(4)
	y	0.2350(4)	0.2340(8)	0.2336(6)	0.2351(4)
	z	0.00	0.00	0.00	0.00
	β_{11}	0.0039(5)	0.0068(11)	0.0079(9)	0.0028(4)
	β_{22}	0.0031(4)	0.0039(10)	0.0041(8)	0.0022(4)
	β_{33}	0.0047(4)	0.0102(10)	0.0090(7)	0.0051(4)
	β_{12}	0.0027(4)	0.0045(9)	0.0042(7)	0.0018(4)
	B(eq)	1.02(5)	1.86(14)	1.92(10)	0.95(5)
O2	x	0.4895(3)	0.4966(6)	0.4974(5)	0.4982(3)
	y	0.1468(3)	0.1456(4)	0.1465(3)	0.1468(2)
	z	0.1445(2)	0.1436(4)	0.1438(3)	0.1447(2)
	β_{11}	0.0034(3)	0.0056(6)	0.0083(5)	0.0038(3)
	β_{22}	0.0041(3)	0.0068(7)	0.0056(5)	0.0040(3)
	β_{33}	0.0025(2)	0.0043(4)	0.0048(3)	0.0026(2)
	β_{12}	0.0024(3)	0.0048(6)	010036(4)	0.0024(3)
	β_{13}	-.0018(2)	-.0015(5)	-.0039(5)	-.0018(2)
	β_{23}	-.0012(2)	-.0004(4)	-.0013(4)	-.0014(2)
	B(eq)	0.86(3)	1.35(8)	1.72(6)	0.91(3)
C(1)	x	0.00	0.00	0.00	0.00
	y	0.00	0.00	0.00	0.00
	z	0.25	0.25	0.25	0.25
	β_{11}	0.0068(5)	0.0133(16)	0.0272(20)	0.0067(5)
	β_{22}	β_{11}	β_{11}	β_{11}	β_{11}
	β_{33}	0.0043(6)	0.0080(15)	0.0106(16)	0.0052(6)
	β_{12}	½β_{11}	½β_{11}	½β_{11}	½β_{11}
	B(eq)	1.65(9)	3.18(27)	5.87(29)	1.73(9)
C(2)	x	0.00	0.00	0.00	0.00
	y	0.00	0.00	0.00	0.00
	z	0.00	0.00	0.00	0.00
	β_{11}	0.0005(12)	-.0083(42)	0.0002(20)	010059(18)
	β_{22}	β_{11}	β_{11}	β_{11}	β_{11}
	β_{33}	0.0096(29)	0.0034(39)	0.0293(80)	0.0029(19)
	β_{12}	½β_{11}	½β_{11}	½β_{11}	½β_{11}
	B(eq)	1.17(32)	1.80(56)	3.38(50)	1.34(39)

[1] After heating.

[2] Numbers in parentheses represent the estimated standard error ($1\hat{\sigma}$) in the last decimal place.

[3] Equivalent isotropic temperature factors (Å^2) were calculated using the expression of Hamilton (1959).

Results and discussion

Structure and channel constituents

The room-temperature structure of Cs- and Li-rich beryl from the Harding pegmatite (HB-3) is similar to the structure of hydrous and anhydrous synthetic beryls studied by Gibbs et al. (1968) and Morosin (1972) and is virtually identical to the structure of a Cs- and Li-rich

Table 5. Selected bond distances and angles[1] for beryl HB-3 at three temperatures

	(24°C)	(500°C)	(800°C)	(24°C after heating)
Interatomic distances in SiO_4 tetrahedron				
Si-O1	1.611(3)[2]	1.617(6)	1.615(5)	1.608(3)
Si-O1	1.603(3)	1.607(6)	1.608(4)	1.608(3)
Si-O2 (2 bonds)	1.614(2)	1.605(4)	1.611(3)	1.615(2)
O1-O1	2.559(4)	2.550(7)	2.553(5)	2.559(3)
O1-O2 (2 bonds)	2.615(3)	2.608(7)	2.622(5)	2.615(3)
O2-O2	2.671(4)	2.659(8)	2.665(6)	2.675(4)
Mean Si-O distance	1.610(3)	1.608(5)	1.611(4)	1.611(3)
O-Si-O angles in SiO_4 tetrahedron				
O1-Si-O2	108.33(10)	108.04(22)	108.74(16)	108.47(10)
O2-Si-O1	111.32(11)	111.78(20)	111.28(16)	111.18(10)
O1-Si-O1	105.58(25)	104.74(53)	104.93(40)	105.44(23)
O2-Si-O2	111.69(18)	112.04(36)	111.59(28)	111.83(18)
Interatomic distances in BeO_4 tetrahedron				
Be-O2 (4 bonds)	1.675(2)	1.681(4)	1.686(3)	1.675(2)
O2-O2 (2 bonds)	2.724(4)	2.724(8)	2.738(6)	2.728(4)
O2-O2	2.393(4)	2.422(8)	2.417(6)	2.391(4)
O2-O2	3.050(4)	3.053(9)	3.064(6)	3.049(4)
O-Be-O angles in BeO_4 tetrahedron				
O2-Be-O2	91.20(14)	91.90(31)	91.61(21)	91.09(14)
O2-Be-O2	108.75(14)	108.49(28)	108.55(21)	108.95(14)
O2-Be-O2	131.11(15)	130.51(33)	130.83(25)	131.01(15)
Interatomic distances in M_1O_6 octahedron				
M-O2 (6 bonds)	1.913(2)	1.931(5)	1.925(3)	1.912(2)
O2-O2 (2 bonds)	2.393(4)	2.422(8)	2.417(6)	2.391(4)
O2-O2 (2 bonds)	2.717(4)	2.738(8)	2.729(6)	2.712(4)
O2-O2 (2 bonds)	2.851(4)	2.877(8)	2.866(6)	2.850(4)
Angles in M_1O_6octahedron				
O2-M-O2	77.47(13)	77.50(24)	77.93(18)	77.46(46)
Ow-M-O2	96.30(9)	96.41(17)	96.12(13)	96.37(9)
O2-M-O2	90.52(13)	90.24(26)	90.37(21)	90.38(13)
Interatomic distances in $C(1)O_{12}$ site				
C(1)-O1 (12 bonds)	3.448(3)	3.444(5)	3.447(4)	3.448(2)
Angles in $C(1)O_{12}$ site				
O1-C(1)-O1	43.58(3)	43.47(6)	43.48(4)	43.57(3)
O1-C(1)-O1	80.03(6)	79.80(12)	79.82(9)	80.00(5)
O1-C(1)-O1	95.88(8)	95.55(16)	95.60(12)	95.84(7)
Interatomic distances in $C(2)O_8$ site				
C(2)O1 (6 bonds)	2.559(4)	2.550(7)	2.553(5)	2.559(3)
C(2)-C(1) (2 bonds when Na in C(2) and H_2O in C[1])	2.311(0)	2.315(0)	2.316(0)	2.311(0)
Angles in $C(2)O_8$ site				
O1-C(2)-O1	60.00	60.00	60.00	60.00
O1-C(2)-O1	120.00	120.00	120.00	120.00
O1-C(2)-O1	180.00	180.00	180.00	180.00
C(1)-C(2)-C(1)	180.00	180.00	180.00	180.00

[1] *Distances are in angstroms and angles are in degrees.*

[2] *Numbers in parentheses represent the estimated standard error* [$1\hat{\sigma}$] *in the last decimal place.*

beryl from the Tanco pegmatite (Manitoba) reported by Hawthorne and Černý (1977) (Table 7). Therefore, the discussion below will focus on channel constituents.

Cs^+, K^+, Na^+, and Ca^{2+} ions and neutral water molecules occupy channel positions in Harding beryl. Water was placed in the C(1) site following the work of Gibbs et al. (1968). Size constraints were used to assign the larger Cs^+ and K^+ ions to the larger C(1) site and the smaller Na^+ and Ca^{2+} to the smaller C(2) site. Featureless difference Fourier maps resulted from these site assignments, which are similar to those made by Evans and Mrose (1968) and Hawthorne and Černý (1977).

Table 7. Comparison of average bond lengths in anhydrous, hydrous, and alkali beryl

Reference		<T1-O>	<T2-O>	<M-O>	<C(1)-O>	<C(2)-O>
This study	(24°C)	1.610(3)[1]	1.675(2)	1.913(2)	3.448(3)	2.559(4)
	(500°C)	1.609(5)	1.681(4)	1.931(5)	3.444(5)	2.555(7)
	(800°C)	1.609(4)	1.686(3)	1.925(3)	3.447(4)	2.555(5)
	(24°C AH)[2]	1.611(3)	1.675(2)	1.912(2)	3.448(2)	2.559(3)
Gibbs *et al.* (1968)						
	Hydrous beryl	1.611(4)	1.654(3)	1.903(3)	...	...
	Anhydrous beryl	1.607(4)	1.660(3)	1.903(3)	...	...
Morosin (1972)						
	Hydrous beryl	1.607(1)	1.653(1)	1.904(1)	...	...
Hawthorne & Černý						
(1977)	Alkali beryl	1.608(4)	1.677(3)	1.906(3)	3.439(3)	2.548(5)

[1]*Bond lengths in angstroms. The numbers in parentheses after the bond lengths refer to the standard error (1$\hat{\sigma}$).*
[2]*After heating to* 800°C.

Water within the structure of hydrous beryl has been classified as two different types (Wood and Nassau, 1967) depending on the orientation of the C_2 symmetry axis of the water molecule relative to the **c** axis of beryl. Type I water has its C_2 axis perpendicular to the **c** axis of beryl, whereas Type II water has its symmetry axis parallel to **c**. In both cases, water is weakly bound to O(1) oxygens. Figure 1 illustrates possible positions for hydrogen bonding within the channels of the beryl structure. Wood and Nassau proposed that Type I water occurs when there are no alkali ions in the adjacent C(2) positions and that Type II water exists when there are, as shown schematically in Figure 1. Polarized IR spectra of a sample of HB-3 (G. Rossman, 1977, pers. comm.) showed the presence of both types of water molecules with Type II strongly predominating. This result is consistent with the high alkali content and with Wood and Nassau's observation that a positive correlation exists between Type II water and alkali content in beryls. The distance between the C(1) and C(2) sites, 2.311 Å, is apparently too short to permit Type II water in C(1) sites adjacent to filled C(2) sites. However, Type II water in an adjacent C(1) site aids in balancing the charge of (Na,Ca) occurring in 23% of the C(2) sites in the structure; bond-strength sums (after method of Brown and Shannon, 1973) for $(Na,Ca)O_6$ and $(Na,Ca)O_6H_2O$ are 0.78 and 1.01, respectively. Although Hawthorne and Černý (1977) recognized the charge-balance problem resulting from bonding a second water molecule to Na (Σ bond strengths = 1.24), they hypothesized that Na^+ ions in the C(2) sites are bonded to two water molecules, based on a 2:1 $H_2O:Na^+$ correlation that they obtained from consideration of available hydrous alkali beryl analyses. In light of this 2:1 ratio for beryl as well as the 2:1 ratio of Type II water to "C(2) type" cations in hydrous alkali cordierites (Goldman et al., 1977), we suggest that the 0.23 (Na,Ca) cations per C(2) site in HB-3 are bonded to 0.46 Type II water molecules; this interpretation leaves 0.09 Type I water molecules in C(1) sites with no adjacent C(2) cations. This speculation is consistent with the high proportion of Type II water indicated by Rossman's polarized IR results. In spite of these supporting data, the problem of charge balance at the C(2) site with water molecules in both adjacent C(1) sites remains unexplained.

When Cs^+, K^+, or Rb^+ occur in the C(1) site, it is unlikely that Na^+ occurs in either of the adjacent C(2) sites because of repulsions resulting from the short C(1)–C(2) bond. In view of the 31% vacancy content of C(1) sites per formula unit of HB-3, it is likely that the 0.23 (Na,Ca) occupy C(2) sites with no adjacent C(1) cations or water molecules. If we assume that the 0.23 (Na,Ca) are bonded to 0.46 Type II water molecules, 0.09 Type I water plus 0.14 (Cs,K) occupy C(1) sites that have no adjacent C(2) cations. In order to maintain local charge balance within the structure, it is also possible that Li^+ occurs in T2 sites either above or below filled C(2) sites and adjacent to C(1) sites filled by (Ca,K) as shown in Figure 1. The coupled substitutions $Li^+ + Na^+ = Be^{2+}$ and $Li^+ + (Cs^+,K^+) = Be^{2+}$

Table 8. Percent thermal expansion for Harding beryl (HB-3)

Temperature (°C)		%Δa [1]	%Δc [2]	%ΔV [3]
24°		0.0	0.0	0.0
200°		0.054	0.065	0.176
300°		0.087	0.076	0.249
400°		0.141	0.119	0.410
500°		0.162	0.151	0.483
500°	(after 96 hours)	0.108	0.087	0.307
600°		0.184	0.141	0.512
700°		0.217	0.173	0.614
800°		0.249	0.195	0.703
500°	(after heating)	0.097	0.065	0.264
24°	(after heating)	-0.032	-0.032	-0.088

[1] $100(a_t - a_{24})/a_{24}$
[2] $200(c_t - c_{24})/c_{24}$
[3] $100(V_t - V_{24})/V_{24}$

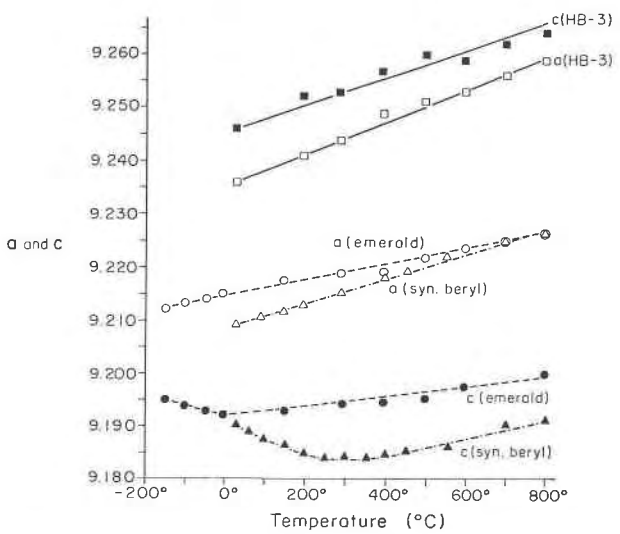

Fig. 2. Variation of cell dimensions with temperature for Harding beryl HB-3, synthetic hydrous beryl, and emerald. Data for the last two are from Morosin (1972).

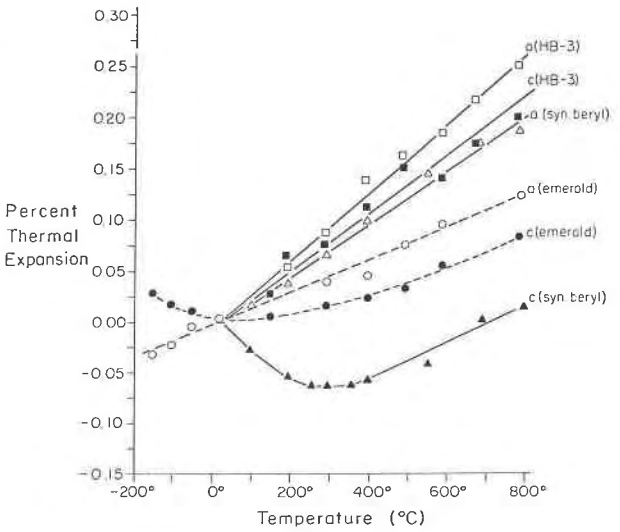

Fig. 3. Percent thermal expansion versus temperature for Harding beryl HB-3, synthetic hydrous beryl, and emerald. Data for the last two are from Morosin (1972).

are consistent with the total channel alkali of 0.37 and tetrahedral Li^+ of 0.38 per formula unit.

Structural formula

Based on the chemical, structural, and IR spectral data and on the crystal chemical reasoning presented above, the following structural formula for Harding beryl HB-3 is proposed:

$$\overbrace{[W(I)_{0.09}W(II)_{0.46}Cs_{0.09}K_{0.05}\square_{0.31}]^{XII}}^{C(1)}$$

$$\overbrace{[Na_{0.21}Ca_{0.02}Mg_{0.02}Fe^{3+}_{0.01}\square_{0.74}]^{VI}}^{C(2)}$$

$$\overbrace{[Al_{2.0}]^{VI}}^{M} \quad \overbrace{[Be_{2.59}Li_{0.38}Al_{0.02}]^{IV}}^{T2}$$

$$\overbrace{[Si_{5.92}Al_{0.08}]^{IV}}^{T1} O_{18},$$

where W(I) and W(II) refer to Type I and Type II water, respectively, and □ refers to vacancies. The small amounts of Mg^{2+} and Fe^{3+} indicated by Peck and Steven's analysis (Table 1) are assigned to C(2), and the 0.02 excess Al^{3+} ions are assigned to T2 to compensate for the slight cation deficiency there. The significance of the Mg and Fe assignments is uncertain because the amounts of these cations approach the detection limits of the wet chemical analysis. The calculated density, 2.72 g/cm³, based on this formula, agrees well with that measured, 2.71 g/cm³, by Berman balance.

High-temperature crystal chemistry

Thermal expansion. The variation of *a* and *c* with increasing temperature for HB-3 is listed in Table 8; comparisons of absolute and percentage changes in *a* and *c* for synthetic beryl and emerald (Morosin, 1972) and HB-3 are shown in Figures 2 and 3. In each case, *a* increases in a linear fashion; however, *c* initially contracts then expands in synthetic beryl and emerald but expands over the same temperature range for HB-3. The *c* cell parameter is smaller than *a* at all temperatures for the two synthetic beryls but is larger than *a* for HB-3. The variation of cell parameters with temperature for low-alkali cordierites (Hochella et al., 1979; Evans et al., 1980) is similar to that for low-alkali or alkali-free beryls with *c* contracting and *a* expanding. All available data for beryl and cordierite indicate that cell volume increases uniformly with temperature.

Thermal expansion coefficients, ϵ_1 and ϵ_3, were calculated for HB-3 using linear and second-order polynomal fits to *a* and *c*, respectively. These values for alkali-rich beryl, synthetic beryl, and emerald over the range 24–800°C are listed in Table 9. Figure 4 shows the variation of ϵ_1, ϵ_3 and β for HB-3, synthetic beryl, and indialite. In each, ϵ_1 is constant as a function of temperature and, for beryl, decreases in magnitude as the composition becomes more complex. The ϵ_3 and β values for indialite vary nonlinearly with temperature, whereas these values for both beryls show a linear dependence on temperature. The most striking difference between the coefficients for HB-3 and synthetic beryl and indialite is the uniformly negative slope in ϵ_3 and β with varying temperature for HB-3 versus the positive slopes for the latter two.

The differences in thermal expansion behavior discussed above are related to composition and bond strengths. Morosin (1972) discussed the effects of small amounts of Cr^{3+} impurity on the thermal expansion behavior of beryl and noted a 200°C shift in the minimum of the *c*-axis expansion. This observation was rationalized by Schlenker et al. (1977) as being due to the strong in-

Table 9. Thermal expansion coefficients ($°C^{-1}$) for Harding beryl, synthetic beryl,[1] and emerald[1]

Temperature		24°	100°	200°	300°	400	500°	600°	700°	800°
ε_1	HB-3	1.2	1.2	1.2	1.2	1.2	1.2	1.2	1.2	1.2
	Synthetic beryl	2.6	2.6	2.6	2.6	2.6	2.6	2.6	2.6	2.6
	Emerald	1.69	1.69	1.69	1.69	1.69	1.69	1.69	1.69	1.69
ε_3	HB-3	3.1	...	2.8	2.5	2.3	2.1	1.9	1.7	1.5
	Synthetic beryl	-3.1	-2.2	-1.4	-0.5	0.4	1.2	2.1	3.0	3.9
	Emerald	-0.4	-0.1	0.4	0.7	1.1	1.4	1.8	2.2	2.5
β	HB-3	8.3	...	8.0	7.7	7.5	7.3	7.1	6.9	6.7
	Synthetic beryl	2.1	3.0	3.8	4.7	5.6	6.4	7.3	8.2	9.0
	Emerald	3.0	3.4	3.7	4.1	4.4	4.8	5.2	5.5	5.8

[1] *From Schlenker et al. (1977). All values of* ε_1, ε_3, *and* β *are* $\times 10^{-6}$. ε_1, ε_3, *and* β *were calculated using the following equations:* $\varepsilon_1 = 1/a_T\ (2.9711 \times 10^{-5})$; $\varepsilon_3 = \dfrac{c_1 + 2c_2T}{c_0 + c_1T + c_1T^2}$, *where* $c_0 = 9.2461$, $c_1 = 2.9524 \times 10^{-5}$, *and* $c_2 = -1.0 \times 10^{-8}$ $\beta = 2\,\varepsilon_1 + \varepsilon_3$

fluence exerted by Cr^{3+} on the strain dependence of the frequencies of the normal modes of beryl. They further demonstrated that positive expansion along **a** and **c** in beryl can occur only when the ratio of the Gruneisen parameters, γ_1 and γ_3, satisfies the following inequality:

$$\frac{S_{11} + S_{12}}{|S_{13}|} > \frac{\gamma_3}{\gamma_1} > \frac{2|S_{13}|}{S_{33}}, \qquad (1)$$

where the S_{ij} values are elastic compliance coefficients for beryl and γ_1 and γ_3 are measures of the thermodynamic driving force of thermal expansion. When γ_3/γ_1 drops below the lower limit, *c* should contract, whereas *a* should contract when the upper limit is exceeded. Experimental values for the ratios $(S_{11} + S_{12})/|S_{13}|$ and $2|S_{13}|/S_{33}$ of 2.39 and 0.54, respectively, were determined by Yoon and Newnham (1973) for beryl and are not sensitive to small compositional changes.

Values of γ_3/γ_1 for HB-3, synthetic beryl, and emerald are listed in Table 10 and plotted in Figure 5. In contrast with the γ_3/γ_1 ratios for synthetic beryl and emerald—which drop below the lower limit of the above inequality at 388 and 130°C, respectively, and which correlate positively with increasing temperature—the curve of γ_3/γ_1 versus temperature for HB-3 has a negative slope and satisfies the inequality over the temperature range 24–800°C. The experimental ϵ_3 values of Harding beryl are thus consistent with the thermodynamic requirements for positive expansion along **c** and **a**. Finally, the curves for

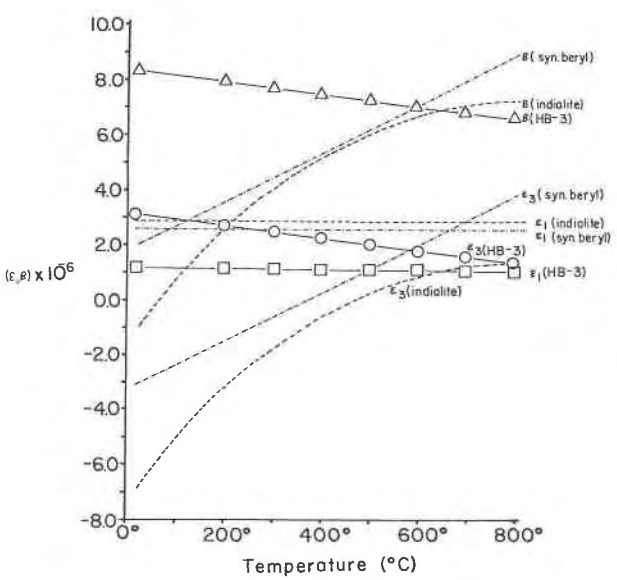

Fig. 4. Variation of thermal expansion coefficients ϵ_1 (along **a**), ϵ_3 (along **c**), and β (volume) with temperature for Harding beryl HB-3, synthetic beryl (Morosin, 1972), and indialite (Evans et al., 1980).

Table 10. Ratio of Gruneisen parameters, γ_3/γ_1, for synthetic beryl, emerald, and Harding beryl at different temperatures

Temperature (°C)	γ_3/γ_1 (HB-3)	γ_3/γ_3 (Syn. Beryl)[1]	γ_3/γ_1 (Emerald)[1]
24°	1.30	-0.33	0.40
100°	-	-0.05	0.55
200°	1.25	0.25	0.65
300°	1.21	0.45	0.75
400°	1.17	0.60	0.85
500°	1.13	0.75	0.90
600°	1.09	0.85	0.95
700°	1.05	0.95	1.00
800°	1.01	1.05	1.05

[1] *From Schlenker et al. (1977).* $\gamma_3/\gamma_1 = \dfrac{2\varepsilon_1 + 2.39\,\varepsilon_3}{3.7037\,\varepsilon_1 + \varepsilon_3}$

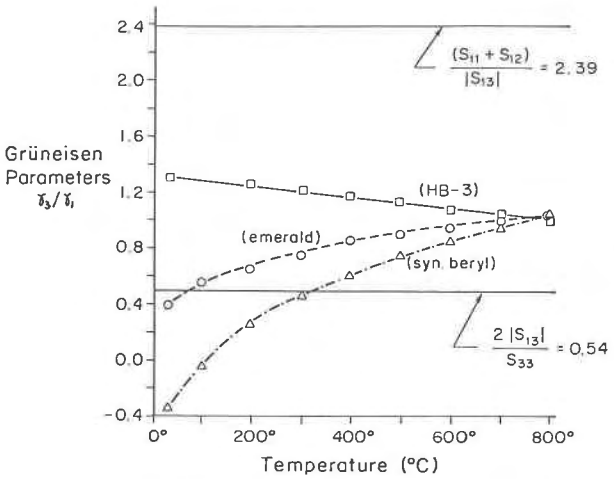

Fig. 5. Ratio of Gruneisen parameters, γ_3/γ_1, versus temperature for Harding beryl HB-3, synthetic beryl, and emerald. These values for the last two are from Schlenker et al. (1977).

all three beryls converge to a common value of γ_3/γ_1 at high temperatures.

Polyhedral distances and volume changes. Mean T1–O, C(1)–O, and C(2)–O distances are constant from 24 to 800°C, whereas mean T2–O and M–O distances increase slightly (Table 5). In spite of the constancy of T1–O, C(1)–O and C(2)–O distances, the volume of the C(1) hexagonal antiprism decreases with increasing temperature (Table 11); the T1 tetrahedral volume is constant, but the T2 and M polyhedra increase in volume. Examination of individual distances and T1–O–T1 and O(1)–T1–O(1) angles (Table 5) indicates that the hexagonal silicate rings remain rigid with increasing temperature. However, the constancy of C(1)–O(1) distances with increasing temperature does not constrain the $C(1)O_{12}$ polyhedral volume to constancy or prevent vertically adjacent silicate rings from moving relative to one another. In fact, the $C(1)O_{12}$ polyhedron decreases in volume from 24 to 500°C and remains essentially constant in volume from 500 to 800°C. This behavior can be rationalized by noting that the O(1)–C(1)–O(1) angle decreases from 24 to 500°C and remains essentially constant from 500 to 800°C. M–O bonds exhibit the largest absolute expansion as do MO_6 octahedral volumes over the temperature range 24–500°C. However, it should be noted that M–O bond lengths (Table 5) and MO_6 bond volume (Table 11) decrease slightly from 500 to 800°C.

Structural interpretation of thermal expansion. The structural manifestations of linear thermal expansion along the **a** and **c** axes of beryl-cordierite–type framework silicates are (1) an increase in the size of the MO_6 octahedron and, in beryl, the $T2O_4$ tetrahedron; (2) changes in the T–O–M and O–T–O angles; (3) a rotation of nonring T2 tetrahedra about axes lying in (001); and (4) rotation of vertically adjacent six-membered rings in opposite senses about [001]. In White Well cordierite, thermal expansion behavior can be adequately explained by expansion of M octahedra coupled with changes in O–T–O and T–O–M bond angles (Hochella et al., 1979). The T1 and T2 tetrahedra, occupied by Si^{4+} and Al^{3+}, have essentially constant volumes and constant T–O bond distances with increasing temperature. Expansion of M octahedra under these circumstances is accompanied by changes in O–T–O and T–O–M angles. Because the M octahedron contributes largely to expansion in the **a** and **b** directions, those O–T–O angles allowing expansion of the framework in these directions must increase with a corresponding decrease in O–T–O angles contributing to the *c* cell dimension. The result is a net decrease in *c* with increasing temperature.

Table 11. Polyhedral volumes (Å³) for beryl HB-3: T1, T2, M, and C(1) sites

Temperature (°C)	T1	T2	M	C(1)
24°	2.14	2.11	9.07	122.06
500°	2.13	2.16	9.35	108.25
800°	2.14	2.16	9.26	108.56
24° (after heating)	2.14	2.11	9.09	134.94

Beryl has T2 tetrahedra occupied by Be^{2+} and Li^+ when present. T2–O bonds expand significantly ($\bar{\alpha}_{T2\text{–}O} = 8.4 \times 10^{-6}$ °C^{-1} for HB-3) and at a rate predicted to increase as Li^+ increasingly substitutes for Be^{2+}. Another difference between beryl and cordierite involves the expansion of M octahedra. For the Mg octahedron in cordierite, $\bar{\alpha}_{M\text{–}O} = 12.6 \times 10^{-6}$ °C^{-1} (Hochella et al., 1979), whereas for the Al octahedron in HB-3, $\bar{\alpha}_{M\text{–}O} = 9.1 \times 10^{-6}$ °C^{-1} over the range 24–800°C. This latter value is similar to the average Al–O bond expansion observed in oxides ($\bar{\alpha} = 8.8 \times 10^{-6}$ °C^{-1}; Hazen and Prewitt, 1977). On the average, both T2 and M polyhedra expand with increasing temperature in HB-3. Even though O–T–O and T–O–M angles behave similarly to those in cordierite, expansion occurs along both **a** and **c** in this beryl. The differences in thermal expansion behavior among Harding beryl, White Well cordierite, and other beryl-cordierite structure types are thus due to differences in T2 and M polyhedral expansion. For example, the differences in expansivity along **c** between alkali-free beryl (Morosin, 1972) and the alkali-rich Harding beryl correlates with the Li content of the T2 tetrahedron and the presence of channel cations in the latter.

Concomitant with changes in the dimensions of the $T2O_4$ and MO_6 polyhedra and in O–T–O and T–O–M bond angles in HB-3, the vertically adjacent six-membered rings rotate slightly in opposite senses about **c**. This phenomenon was also observed in White Well cordierite; the rings move such that T1 tetrahedra in vertically adjacent rings, which are linked to the same T2 tetrahedron, rotate in opposite directions around **c** (0.2° from 24 to 775°C; Hochella et al., 1979). In this case, the rotation was attributed to expansion of the M octahedron. In HB-3, two different modes of rotation about **c** by the six-membered rings were observed, although the magnitudes are comparable to the calculated standard errors of bond

angles. The first, occurring from 24 to 500°C, was rotation in the opposite sense to that observed in cordierite (0.2° from 24 to 500°C), whereas from 500 to 800°C, the rings rotated (0.4°) in the same sense as observed in cordierite. The expansion along **c** from 24 to 500°C is dominated by T2 tetrahedral expansion, which causes the rings to rotate in the opposite sense to that observed in cordierite. From 500 to 800°C, M-octahedral-volume change dominates.

Effects of heat treatment. Only slight differences between the beryl structures before and after heating to 800°C were observed. The conventional *R* factors from the two 24°C refinements are identical (0.050), although standard errors are slightly better for the 24°C structure after heating. In the higher-temperature refinements, electron density in the channel sites becomes more diffuse, consistent with high thermal motion (Table 4) and in a manner proportional to the ratio of electron densities of the C(1) and C(2) sites in the 24°C structure. However, when the temperature was reduced to 24°C after heating at 800°C for 72 h, the electron densities at the C(1) and C(2) sites returned to their values prior to the initial heating; suggesting that little net change occurred in channel constituents during the high-temperature experiments. Our suggestion is consistent with the results of TGA measurements on a sample of Harding beryl (B. Chakuomakos, 1985, pers. comm.) that indicate only 0.15 wt% loss at 800°C. These results differ somewhat from the findings of Aines and Rossman (1984), who reported some dehydration of their beryl after heat treatment at 700°C for 2 h. Because they did not report alkali contents, it is not possible to reconcile these findings. Positional parameters and bond lengths and angles were also essentially unchanged before and after heating. In this regard, the difference in C(1) polyhedral volumes before and after heating (Table 11) is anomalous. Our result differs from the observed loss of channel water after several days at 775°C in White Well cordierite. This difference is due to the presence of significant amounts of Na^+, Cs^+, and K^+ in HB-3, which apparently "plug" the channels, and to their absence in White Well cordierite.

Acknowledgments

We wish to thank the late R. H. Jahns (Stanford University) for providing the chemically analyzed sample of Harding beryl used in this study, and we are grateful to George Rossman (California Institute of Technology) for running polarized IR spectra of this beryl and for helpful discussions concerning channel constituents in beryl-cordierite–type framework silicates. We also wish to thank K. D. Keefer (Sandia National Laboratories) and M. P. Taylor (Corning Glass Works) for help with various aspects of the computer work and B. Chakoumakos (University of New Mexico) for carrying out TGA measurements on a sample of Harding beryl. M. F. Hochella, Jr. (Stanford), Joan R. Clark (formerly with the USGS), B. Chakoumakos, and an anonymous reviewer are thanked for critical reviews of the manuscript. This study was supported by the Experimental and Theoretical Geochemistry Program of the National Science Foundation through Grant EAR-80-16911 (Brown).

References

Aines, R.D., and Rossman, G.R. (1984) The high temperature behavior of water and carbon dioxide in cordierite and beryl. American Mineralogist, 69, 319–327.

Bakakin, V.V., Rylov, G.M., and Belov, N.V. (1969) Crystal structure of a lithium-bearing beryl. Akademie Nauk SSSR Doklady, 188, 659–662.

Brown, G.E., Jr., Sueno, S., and Prewitt, C.T. (1973) A new single-crystal heater for the precession camera and four-circle diffractometer. American Mineralogist, 58, 698–704.

Brown, I.D., and Shannon, R.D. (1973) Empirical bond-strength–bond-length curves for oxides. Acta Crystallographica, A29, 266–282.

Carson, D.G., Rossman, G.R., and Vaughan, R.W. (1982) Orientation and motion of water molecules in cordierite: A proton nuclear magnetic resonance study. Physics and Chemistry of Minerals, 8, 14–19.

Corfield, R., Doedens, R.J., and Ibers, J.A. (1967) The crystal and molecular structure of nitrododichlorobis (triphenylphosphine) rhenium (V), $ReNC_2(P(C_6H_5)_3)_2$. Inorganic Chemistry, 6, 197–204.

Doyle, P.A., and Turner, P.S. (1968) Relativistic Hartree-Fock X-ray and electron scattering factors. Acta Crystallographica, A24, 390–397.

Evans, D.L., Fischer, G.R., Geigher, J.E., and Martin, F.W. (1980) Thermal expansion and chemical modifications of cordierite. American Ceramic Society Journal, 63, 629–634.

Evans, H.T., Jr., and Mrose, M.E. (1968) Crystal chemical studies of cesium beryl. Geological Society of America Special Paper 101, Abstracts for 1966, 63.

Filho Sampaio, H. de Almeido, Sighinolfi, G.P., and Galli, E. (1973) Contributions to the crystal chemistry of beryl. Contributions to Mineralogy and Petrology, 38, 279–290.

Finger, L.W., and Prince, E. (1975) A system of FORTRAN IV computer programs for crystal structure computations. United States Department Commerce, National Bureau of Standards Technical Note 854.

Gibbs, G.V., Breck, D.W., and Meagher, E.P. (1968) Structural refinement of hydrous and anhydrous synthetic beryl $Al_2(Be_3Si_6)O_{18}$ and emerald, $Al_{1.9}Cr_{0.1}(Be_3Si_6)O_{18}$. Lithos, 1, 275–285.

Goldman, D.S., Rossman, G.R., and Dollase, W.A. (1977) Channel constituents in cordierite. American Mineralogist, 62, 1144–1157.

Goldman, D.S., Rossman, G.R., and Parkin, K.M. (1978) Channel constituents in beryl. Physics and Chemistry of Minerals, 3, 225–235.

Hamilton, W.C. (1959) On the isotropic temperature factor equivalent to a given anisotropic temperature factor. Acta Crystallographica, 12, 609–610.

Hawthorne, F.C., and Černý, P. (1977) The alkali-metal positions in Cs-Li beryl. Canadian Mineralogist, 15, 414, 421.

Hazen, R.M., and Prewitt, C.T. (1977) Effects of temperature and pressure on interatomic distances in oxygen-based minerals. American Mineralogist, 62, 309–316.

Hochella, M.F., Jr., Brown, G.E., Jr., Ross, F.K., and Gibbs, G.V. (1979) High temperature crystal chemistry of hydrous Mg and Fe rich cordierites. American Mineralogist, 64, 337–351.

Jahns, R.H., and Ewing, R.C. (1976) The Harding mine, Taos County, New Mexico. New Mexico Geological Society Guidebook, 27th Field Conference, Vermejo Park, 263–276.

———(1977) The Harding mine. Mineralogical Record, 8, 115–126.

MacGillavry, C.H., and Rieck, G.D. (1968) International tables for X-ray crystallography, volume III, 202–205.

Morosin, Bruno. (1972) Structure and thermal expansion of beryl. Acta Crystallographica, B28, 1899–1903.

Price, D.C., Vance, E.R., Smith, G., Edgar, A., and Dickson, B.L. (1976) Mossbauer effect studies of beryl. Journal de Physique,

Colloque C6, supplement au no. 12, Tome 37, Decembre, C6-811–C6-817.
Schaller, W.T., Stevens, R.E., and Jahns, R.H. (1962) An unusual beryl from Arizona. American Mineralogist, 47, 672–699.
Schlenker, J.L., Gibbs, G.V., Hill, R.G., Crews, S.S., and Myers, R.H. (1977) On the relation between negative thermal expansion, strain dependence of entropy and elasticity in indialite, emerald and beryl. Physics and Chemistry of Minerals, 1, 243–255.
Wood, D.L., and Nassau, K. (1967) Infrared spectra of foreign molecules in beryl. Journal of Chemical Physics, 47, 2220–2228.
Yoon, H.S., and Newnham, R.E. (1973) The elastic properties of beryl. Acta Crystallographica, A29, 507–509.

Manuscript received May 24, 1985
Manuscript accepted November 8, 1985